doi:10.1093/brain/awp148 Brain 2009: 132; 2464–2477 | 2464

BRAIN
A JOURNAL OF NEUROLOGY

Accuracy of hippocampal network activity is disrupted by neuroinflammation: rescue by memantine

S. Rosi,[1,2,3] V. Ramirez-Amaya,[4] A. Vazdarjanova,[5] E. E. Esparza,[4] P. B. Larkin,[6,7] J. R. Fike,[1,3] G. L. Wenk[8] and C. A. Barnes[9,10]

1 Brain and Spinal Injury Center, University of California, San Francisco, CA, USA
2 Department of Physical Therapy and Rehabilitation Science, University of California, San Francisco, CA, USA
3 Department of Neurological Surgery, University of California, San Francisco, CA, USA
4 Instituto de Neurobiologia, Universidad Nacional Autonoma de Mexico, Juriquilla, Queretaro, Mexico
5 Medical College of Georgia, Augusta, GA, USA
6 Neuroscience Graduate Program, University of California, San Francisco, CA, USA
7 Gladstone Institute of Neurological Disease, University of California, San Francisco, CA, USA
8 Department of Psychology, Ohio State University, Columbus, OH, USA
9 Arizona Research Laboratories, Neural Systems Memory and Aging, University of Arizona, Tucson, AZ, USA
10 Evelyn F. McKnight Brain Institute, University of Arizona, Tucson, AZ, USA

Correspondence to: S. Rosi, Ph.D.,
Brain and Spinal Injury Center,
San Francisco General Hospital,
Building 1, Room 101,
1001 Potrero Avenue,
San Francisco, CA 94110,
USA
E-mail: rosis@ptrehab.ucsf.edu

Understanding how the hippocampus processes episodic memory information during neuropathological conditions is important for treatment and prevention applications. Previous data have shown that during chronic neuroinflammation the expression of the plasticity related behaviourally-induced immediate early gene *Arc* is altered within the CA3 and the dentate gyrus; both of these hippocampal regions show a pronounced increase in activated microglia. Low doses of memantine, a low to moderate affinity open channel uncompetitive *N*-Methyl-D-aspartate receptor antagonist, reduce neuroinflammation, return *Arc* expression to control levels and attenuate cognitive deficits induced by lipopolysaccharide. Here we investigate whether neuroinflammation affects the accuracy of information processing in the CA3 and CA1 hippocampal regions and if this is modified by memantine treatment. Using the immediate early gene-based brain-imaging method called cellular analysis of temporal activity by fluorescence *in situ* hybridization, it is possible to detect primary transcripts at the genomic alleles; this provides exceptional temporal and cellular resolution and facilitates the mapping of neuronal activity. Here, we use this method to compare the neuronal populations activated by two separate experiences in CA1 and CA3 and evaluate the accuracy of information processing during chronic neuroinflammation. Our results show that the CA3 pyramidal neuron activity is not stable between two exposures to the same environment context or two different contexts. CA1 networks, however, do not differ from control conditions. These data suggest that during chronic neuroinflammation, the CA3 networks show a disrupted ability to encode spatial information, and that CA1 neurons can work independently of CA3. Importantly, memantine treatment is able to partially normalize information processing in the hippocampus, suggesting that when given early during the development of the pathology memantine confers neuronal and cognitive protection while indirectly prevents pathological microglial activation.

Received November 6, 2008. Revised April 23, 2009. Accepted May 2, 2009. Advance Access publication June 16, 2009

Keywords: hippocampal networks; immediate early gene; neuroinflammation; NMDARs modulation

Abbreviations: aCSF = artificial cerebrospinal fluid; *Arc* = activity-regulated cytoskeletal associated protein; catfish = cellular analysis of temporal activity by fluorescence *in situ* hybridization; Cy3 = cyanine 3; LPS = lipopolysaccharide; NMDARs = *N*-Methyl-D-aspartate receptors

Introduction

The chronic neuroinflammation present in the early stages of many neurodegenerative conditions, such as Alzheimer's disease, traumatic brain injury and HIV dementia, may contribute to the severe cognitive decline associated with these disorders (McGeer and McGeer, 1998; Akiyama *et al*., 2000; Morganti-Kossmann *et al*., 2001; Fischer-Smith *et al*., 2004). Activated microglia and their products are key mediators of the neuroinflammatory process that contributes to neuronal damage (Barger and Basile, 2001). There is evidence that during the early stages of Alzheimer's disease, before neuronal degeneration occurs, activated microglia are found in the hippocampal formation, a region that plays a critical role in associative learning and memory (Cagnin *et al*., 2001). Further support for the role of microglia in altered hippocampal function comes from laboratory studies that show that chronic neuroinflammation increases activated microglia in the dentate gyrus and CA3 region and alters the expression of the behaviourally induced immediate early gene (IEG), activity-regulated cytoskeleton-associated protein (*Arc*), in these same regions (Rosi *et al*., 2005, 2006). This may result in altered coupling of neuronal activity with macromolecular synthesis (transcription and translation) implicated in learning and memory (Rosi *et al*., 2005).

Arc is expressed in cortical and hippocampal glutamatergic neurons, and is required for engaging durable plasticity processes that may underlie memory consolidation (Lyford *et al*., 1995; Guzowski *et al*., 2000). For example, reduction in *Arc* through genetic manipulation or antisense oligonucleotides leads to significant hippocampal dependent cognitive dysfunction (Guzowski *et al*., 2000; Plath *et al*., 2006). Following behavioural foraging experiences, *Arc* is activated in hippocampal neurons in proportions similar to those recorded electrophysiologically under similar conditions (Lee *et al*., 2004; Leutgeb *et al*., 2004). The correspondence in circuit dynamics between electrophysiology and measurements of *Arc* has led to the suggestion that expression of this *gene* can serve as a reliable monitor of cellular activity reflecting spatial and contextual information processing (Guzowski *et al*., 1999).

Hippocampal network function is essential for discrimination and retrieval of spatial information and enables effective navigational behaviour. Understanding how the disruption of this function is affected by neuroinflammation is critical for the development treatments/approaches to prevent or attenuate cognitive dysfunctions. It has been previously shown that the low-to-moderate affinity open channel non-competitive *N*-methyl-D-aspartate receptor (NMDAR) antagonist memantine can rescue navigational behaviour during chronic neuroinflammation while preventing activation of microglia (Rosi *et al*., 2006). Given its unique biophysical and pharmacological properties (Parsons *et al*., 1999), memantine at low doses can selectively block pathological influx of calcium ions without affecting the voltage-dependence of NMDAR transmission that is critical for learning and memory. By stochastically blocking open neuronal NMDA channels, memantine may indirectly affect microglial activation. It is not known, however, if the cognitive improvement conferred by memantine is due to restoring proper hippocampal network function, and if memantine affects microglial activation directly or indirectly through neuronal NMDARs.

To study the hippocampal network function during chronic neuroinflammation, we used a novel IEG-based brain-imaging method called cellular analysis of temporal activity by fluorescence *in situ* hybridization (catFISH), which monitors the activity history of neurons after two given learning experiences separated by 30 min. Because the *Arc*-catFISH method requires discrete compartmentalization for localization of mRNA with temporal specificity, and because the dynamics of *Arc* expression are different in the dentate gyrus (Ramirez-Amaya *et al*., 2005), our study only focused on the CA areas. In addition, to determine if memantine acts directly on microglia, we studied its affect on microglial cells in culture.

Methods

Subjects and surgical procedures

Sixty-three, 3-month-old male F-344 (Harlan Sprague–Dawley, Indianapolis, IN, USA) rats were used in this study. All rats were individually caged with food and water freely available. As previously described, artificial cerebrospinal fluid (aCSF, $n = 36$) or lipopolysaccharide (LPS, $n = 29$) (Sigma, St Louis, MO, USA *E. coli*, serotype 055:B5, TCA extraction, 1.0 μg/μl dissolved in aCSF) were loaded into an osmotic minipump (Alzet model #2004, to deliver 0.25 μl/h; Durect Corp., Cupertino, CA, USA) and chronically infused for 28 days through a cannula implanted into the fourth ventricle of the brain (Rosi *et al*., 2005). On the same day of the ventricular implant, a second osmotic minipump was inserted subcutaneously in the back of 14 rats from the lipopolysaccharide infused groups and 16 rats from the aCSF-infused group (Alzet model #2ML4, to deliver 2.5 μl/h) to release subcutaneous memantine (Tocris Bioscience, Ellisville, MO, USA) at a dose of 10 mg/kg/day (Rosi *et al*., 2006). Body weights were determined daily and general behaviour was monitored.

Behavioural procedures

To habituate rats, they were handled daily for 10 days before the novel environment exploration. Twenty-nine days after the initiation of the artificial cerebrospinal fluid, lipopolysaccharide or memantine infusions, the rats were separated in two cohorts: exploration (LPS, $n = 10$; LPS + M, $n = 10$; aCSF, $n = 11$ and aCSF + M, $n = 10$) and caged control (LPS, $n = 5$; LPS + M, $n = 4$; aCSF, $n = 9$; aCSF + M, $n = 6$). Each rat from the exploration cohort was exposed to novel

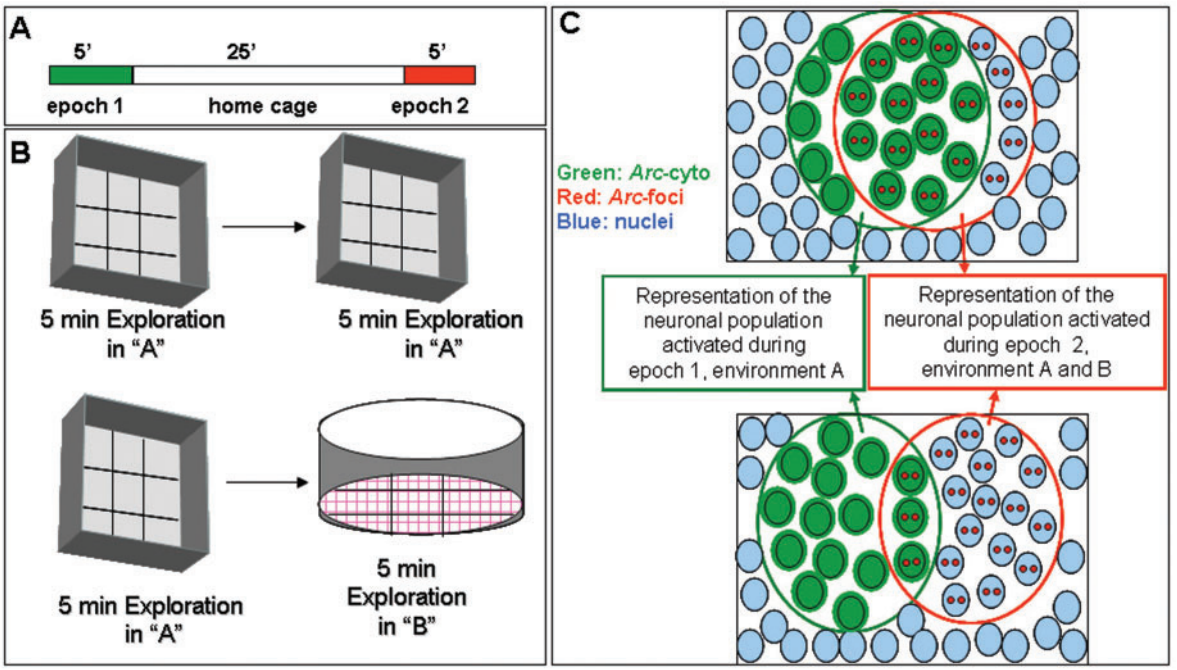

Figure 1 Schematic representation of the experimental procedure (**A**) and types of novel environments (**B**) used in this study. Animals were allowed to explore the novel environment A for 5 min (epoch 1). After 25-min rest period in the home cage, the rats were exposed to either environment A again or environment B (epoch 2). Environment A was an open box (61 × 61cm) with 24-cm high walls. Environment B was a cylinder (75-cm diameter), and was located in a different room than environment A. (**C**) Schematic representation of the neuronal populations that express *Arc* (cytoplasmic, intranuclear foci or both) following exploration of identical (AA, top illustration) or different (AB, bottom illustration) environments. Nuclei are indicated by light blue circles, *Arc* transcription foci (*Arc*-foci) are indicated by two reds spots in the nuclei, cytoplasmic *Arc* mRNA (*Arc*-cyto) is indicated by green coloured nuclei and green shading. The green open circle contains the neuronal population activated during epoch 1 and the red open circle contains the neuronal population activated during epoch 2. The overlap between these two circles represents the neuronal population activated during both epoch 1 and epoch 2. In rats exposed to the same environment twice (AA, top illustration) the majority of *Arc* positive cells contain *Arc*-cyto and *Arc*-foci; indicating that *Arc* activation occurs in the same cell population of neurons during each exposure. Rats exposed to two different environments (AB, bottom illustration) show an equal proportion of stained for *Arc*-cyto or *Arc*-foci and smaller proportion containing both; suggesting that different environments activate independent populations of neurons.

environment A for 5 min (epoch 1), returned to its home cage in the colony room for 25 min, and then exposed for 5 more minutes (epoch 2) either to the same environment (A) or different environment (B; Fig. 1A and B). Environment A was an open box (61 × 61cm) with 24-cm high walls divided into nine grids, and environment B was a cylinder (75 cm diameter, 20 cm high, nine grids) that was located in a different room from environment A but equidistant from the colony room. Between subjects, the environments were cleaned thoroughly with 20% ethyl alcohol (environment A) or 5% bleach (environment B). All behavioural testing was conducted during the dark half of the light/dark daily cycle, which is the active period for rodents. Each rat was manually moved into the centre of a different grid every 15 s in a pseudorandom schedule during the 5-min exploration session. Under this paradigm the proportions of *Arc* expressing neurons was comparable to those obtained with free moving rats (Vazdarjanova and Guzowski, 2004). By manually moving the animals, we reduced the variability and insured that all animals fully explored the environments. Light intensity and distal spatial cues were maintained throughout all behavioural exploration sessions. Immediately after the second exploration session, rats were deeply anaesthetized with isoflurane gas and killed by decapitation. The brain was quickly removed (<120 s) and frozen in −70°C isopentane (2-methyl butane, Sigma). Caged control animals that did not explore the novel environments were killed directly from their home cages interspersed with the rats that were given exploration treatment.

Histological procedures

The brains were divided at the midline and blocked together such that each slide contained sections from one rat from each of the experimental groups (behaviour and non-behaviour, LPS, aCSF and LPS + M, aCSF + M) (Rosi *et al.*, 2006). All slides were cryosectioned and stored at −70°C until processed for immunocytochemistry or fluorescence *in situ* hybridization (FISH).

Immunofluorescence staining

Three slides (containing all the conditions described above) were selected from the medial portion of the dorsal hippocampus (anterior–posterior, ∼−3.6 mm from Bregma) and were stained for activated microglia OX-6 positive, as previously described in detail (Rosi *et al.*, 2005, 2006).

Fluorescence *in situ* hybridization

Sections processed for FISH were prepared and handled as described previously (Vazdarjanova and Guzowski, 2004; Rosi *et al*., 2005, 2006). To unambiguously identify *Arc* transcription induced by the first exploration (epoch 1) and to distinguish it from the recent transcription induced by the second exploration (epoch 2), we used the detection of *Arc* intron riboprobe digoxigenin-labelled and *Arc* full-length riboprobe labelled with fluorescein (for detail see: Guzowski *et al*., 2006). This allowed visualization of the initial transcription (cytoplasmic mRNA form the first exploration) with one fluorophor (FITC, PerkinElmer, Life sciences, Emeryville, CA, USA) and the later transcription (intranuclear foci mRNA from the second exploration) with another fluorophor (cyanine-3, Cy3, PerkinElmer). This approach improves reliability and efficiency and is the basis of the catFISH technique. Digoxigenin- or fluorescein-labelled riboprobes (for *Arc* intranuclear foci and *Arc* full-length probe, respectively) were generated using commercial transcription kits (MaxiScript, Ambion, Austin, TX, USA) and RNA labelling mixes (Roche products, Hertforshire, UK). Briefly, digoxigenin-labelled *Arc* intranuclear foci (*Arc*-foci) was detected with anti-digoxigenin-HRP (Roche products) and was revealed with Cy3. After the detection of *Arc*-foci, the slides were quenched with 2% H_2O_2 to quench the residual HRP activity. Fluorescein-labelled *Arc* full-length probe was then detected with antifluorescein HRP (Roche Products) and revealed with FITC. Nuclei were counterstained with TOPRO (Molecular Probes, Eugene, OR, USA). The control conditions, which were run with no RNA probe, showed no staining.

Image acquisition and analysis

CA3 and CA1 area images were taken using a Zeiss 510 Metaseries laser scanning confocal microscope with a 400X water immersion lens (Thornwood, NY, USA). Three Z-stacks from each brain region (1 μm optical thickness/plane) were imaged and three slides per rat were imaged. Thus, comparable numbers of cells from each rat were analysed. Offline analyses were performed using MetaMorph imaging software (Universal Image Corporation, West Chester, PA, USA) as described previously (Guzowski *et al*., 1999; Vazdarjanova and Guzowski, 2004; Rosi *et al*., 2005, 2006). Neuronal nuclei from the pyramidal cell layers of CA1 and CA3 were classified as negative (containing no transcription foci or cytoplasmic *Arc*), *Arc*-foci positive (containing only *Arc* intranuclear foci staining), *Arc*-cyto positive (containing only cytoplasmic staining) or double-labelled *Arc*-foci/*Arc*-cyto positive (containing both intranuclear foci transcript and cytoplasmic). For analysis, the investigator was blind to the experimental conditions.

Similarity score analysis

When analysing the *Arc* catFISH images it is helpful to reduce the complex cell staining data to a value that can be used to compare cell activity across multiple brain regions. The similarity score takes the four cell staining values defined above (*Arc*-foci, *Arc*-cyto, double-labelled *Arc*-foci/*Arc*-cyto and negative) and reduces them to a single value (Vazdarjanova and Guzowski, 2004). A value of 1 represents a single neuronal population activated in both exploration sessions (epoch 1 and 2). A value of 0 indicates that two statistically independent cell populations were activated during the two exploration sessions (epochs 1 and 2). The similarity score was derived as follows: (i) Epoch 1 active cells = fraction of total *Arc*-positive [(*Arc*-foci/*Arc*-cyto + *Arc*-cyto only)/total cells]; (ii) Epoch 2 active cells = fraction of total fraction of total *Arc*- positive [(*Arc*-foci/*Arc*-cyto +*Arc*-foci only)/total cells]; (iii) p(E1E2) = epoch 1 active cell fraction × epoch 2 active cell fraction. This represents the probability of cells being activated in both epochs (*Arc*-foci/*Arc*-cyto), assuming that the two epochs activated statistical independent neuronal population; (iv) diff(E1E2) = (*Arc*-foci/*Arc*-cyto)-p(E1E2). This represents the measure of the deviation from the independent hypothesis; (v) Least epoch = the smaller of the ensembles activated by epoch 1 or epoch 2; and (vi) Similarity score = diff(E1E2)/(least epoch-p(E1E2)). This normalizes the diff(E1E2) fraction to a perfect condition where A/A is 1 and A/B is 0 (Vazdarjanova and Guzowski, 2004).

Microglia cell culture

N9 microglial cells were cultured in Dulbecco's modified Eagle's medium (DMEM) supplemented with 5% fetal bovine serum and 2% L-glutamine. Cultures were maintained in an incubator at 37°C, 5% CO_2, 95% humidity. Medium was changed every 3–4 days and cells were passaged weekly using 0.05% trypsin. Cells used in all experiments had been passaged fewer than 17 times.

For experiments with LPS and memantine treatment, N9 cells were plated into 24 well plates at 40 000 cells/well in DMEM. Two hours after plating, DMEM was removed and replaced with macrophage serum free medium (MSFM). Twenty-four hours after plating, MSFM was removed and replaced with fresh MSFM containing LPS and/or memantine (LPS 100 ng/mL, memantine 10 or 50 μM). Twenty-four hours after treatment with LPS and/or memantine, cells were lysed and RNA was harvested using a Qiagen RNeasy Mini kit according to the manufacturer's instructions. RNA was immediately reverse transcribed to cDNA using Multiscribe≈ reverse transcriptase (Applied Biosystems). Quantitative real-time PCR (qPCR) was performed using SYBR Green Mastermix (Applied Biosystems) as provided by the manufacturer. qPCR was performed using an ABI Prism 7700 Sequence Detector with the following program: UNG activation (50°C for 2 min), initial denaturation (95°C for 10 min), and then 40 cycles of denaturation (95°C for 15 s) then annealing and extension (60°C for 1 min). Primer specificity was confirmed using melting curve analysis. Amplification efficiency was calculated for each primer pair using serially diluted standards. This efficiency was used to convert cycle threshold (number of PCR cycles required to reach an arbitrary threshold fluorescence value) into relative gene expression. For each sample, expression of the gene of interest was normalized to beta actin expression. Samples run on separate qPCR plates were calibrated to each other using standards that were common to all plates.

Statistical analysis

StatView Softaware was used to perform all the statistical analysis related to catFISH, and Graphpad Prism statistical analysis software was used to analyse gene expression data from four independent experiments. Group differences for the behavioural measures, treatment effect as well as similarity scores, were analysed with ANOVA. When the overall ANOVA was significant ($P < 0.001$) further comparison between groups was done using Bonferroni *post hoc* tests. Only three comparisons, a priori, were planned (aCSF control versus LPS, aCSF + M or LPS + M). For all tests, the null hypothesis was rejected at the 0.05 level of significance.

Results

The immediate early gene-based single cell brain imaging method (*Arc* catFISH) was used to quantitatively assess the reliability of information processing in hippocampal neuronal networks during neuroinflammation and following therapeutic treatment with memantine. The chronic infusion of lipopolysaccharide with or without memantine was well-tolerated by all rats, although there was a transient weight loss over the first few days of treatment. No adverse neurological signs were observed, and counts of CA1 and CA3 neurons revealed no significant changes in the total number of neurons per region in any of the experimental groups when compared to artificial cerebrospinal fluid controls (data not shown). The mean number of neurons analysed for each rat, using the catFISH methods, was 365 ± 18.8 for CA1 and 287 ± 10.3 for CA3.

Operationally, neuronal activation was defined as the fraction of neurons that expressed *Arc* mRNA, either in the nucleus (i.e. foci) or cytoplasm after rats were allowed to explore a given novel environment (Vazdarjanova and Guzowski, 2004; Guzowski *et al*., 2006). The neuronal populations active during two distinct exploration periods (epochs 1 and 2) of either the same (AA) or different (AB) environments were detected using *Arc* catFISH, which allowed the determination of which distinct epoch a given cell was active (Fig. 1C). If the cell was active in the first epoch only, *Arc* expression would be found exclusively only in the cytoplasm (*Arc*-cyto). If the cell was active in the second behavioural epoch only *Arc* expression would be found in the nucleus (*Arc*-foci). If the cell was active in both epochs then *Arc* would be located in both the nucleus and the cytoplasm (*Arc*-foci/*Arc*-cyto).

Nuclei with *Arc*-foci (yellow) can be observed in Figs 2A and 3A, and reflect those cells active within ~5 min of tissue collection. Nuclei containing *Arc*-cyto (green) can be observed in the same figures, which indicate neurons active within ~30 min of tissue collection. Neurons double labelled with both intranuclear and cytoplasmic mRNA (*Arc*-foci/*Arc*-cyto) were active in both exploration sessions (epoch 1 and 2). Therefore, the active cells in epoch 1 are reflected by all the *Arc*-cyto positive neurons (*Arc*-foci/*Arc*-cyto and *Arc*-cyto only) and the active cells in epoch 2 are represented by all the *Arc*-foci positive neurons (*Arc*-foci/*Arc*-cyto and *Arc*-foci only; Fig. 1C).

Lipopolysaccharide affects information processing in CA3 networks: restoration by memantine treatment

To establish how lipopolysaccharide affected network processing, and the subsequent effects of memantine treatment, it was necessary to first determine the numbers of neurons expressing behaviourally induced *Arc*. Under all the experimental conditions used here, the fractions of CA3 neurons expressing *Arc* averaged between 17% and 30% (Fig. 2B), which was significantly higher than the 2.5%–5% observed for caged control animals ($P < 0.001$; data not shown). In animals infused with artificial cerebrospinal fluid, exploration in either the AA or AB environment conditions resulted in similar fractions of activated neurons in both epoch 1 and epoch 2 (Fig. 2B). In lipopolysaccharide-infused animals there was a significant increase in the percentage of *Arc* positive neurons in epochs 1 and 2 and under both exploration conditions compared to artificial cerebrospinal fluid animals [ANOVA: $F(7,38) = 7.5$, $P < 0.001$, for epoch 1; $F(7,38) = 7.1$, $P < 0.001$ for epoch 2; all *post hoc* Bonferroni comparisons $P < 0.05$]. Notably, the proportions of neurons active during AA and AB in epochs 1 and 2 in animals infused with artificial cerebrospinal fluid were similar to those seen in animals infused with aCSF + M and LPS + M (Fig. 2B).

The percentages of neurons active during both epochs were identified by the double-labelled cells (*Arc*-foci/*Arc*-cyto). In rats infused with artificial cerebrospinal fluid, the fraction of double-labelled neurons (active during both epochs 1 and 2) was significantly higher after the AA paradigm compared with the AB exploration group [ANOVA: $F(7,38) = 17$, $P < 0.001$] (Fig. 2C). This suggests that in CA3, the same neurons were activated when the animals explored the same environment twice (AA), but that a statistically independent and smaller group of neurons was activated after exploration of two different environments (AB). A similar relationship was observed in animals infused with aCSF + memantine (Fig. 2C). In contrast, after lipopolysaccharide infusion, the fraction of activated neurons during the AA and AB paradigms was similar (Fig. 2C), while, in LPS-infused rats treated with memantine, the overall response was qualitatively similar to that seen in the two artificial cerebrospinal fluid groups [ANOVA: $F(7,38) = 17$, $P < 0.001$; Fig. 2C].

Information processing in the CA1 area is unaltered by lipopolysaccharide or memantine infusion

For all experimental conditions used here, the fractions of CA1 neurons showing behaviourally induced *Arc* averaged 35%–40%, which was significantly higher than for the caged control animals in which only 5%–6% showed *Arc* expression ($P < 0.001$; data not shown). Similar to what was observed in CA3, exploration (AA or AB) resulted in the activation of a similar percentage of neurons during epochs 1 and 2 for all treatment conditions [ANOVA: $F(7,38) = 3.8$, $P < 0.02$ for epoch 1; $F(7,38) = 1.5$, $P < 0.24$ for epoch 2, Fig. 3B]. When considering only double-labelled cells activated by the two exploration sessions (*Arc*-foci/*Arc*-cyto) the fraction of activated neurons after the AA paradigm was significantly higher than that seen in animals from the AB paradigm in all treatment conditions [ANOVA: $F(7,38) = 35.8$, $P < 0.001$; Fig. 3C], suggesting normal information processing in the CA1 region even during neuroinflammation.

Similarity score

The per cent of double-labelled neurons activated during epochs 1 and 2 (Figs 2C and 3C) can be expressed in summary form using a similarity score analysis that normalizes activity values to range from 0 to 1 (Fig. 4A; see Methods section). Similarity scores

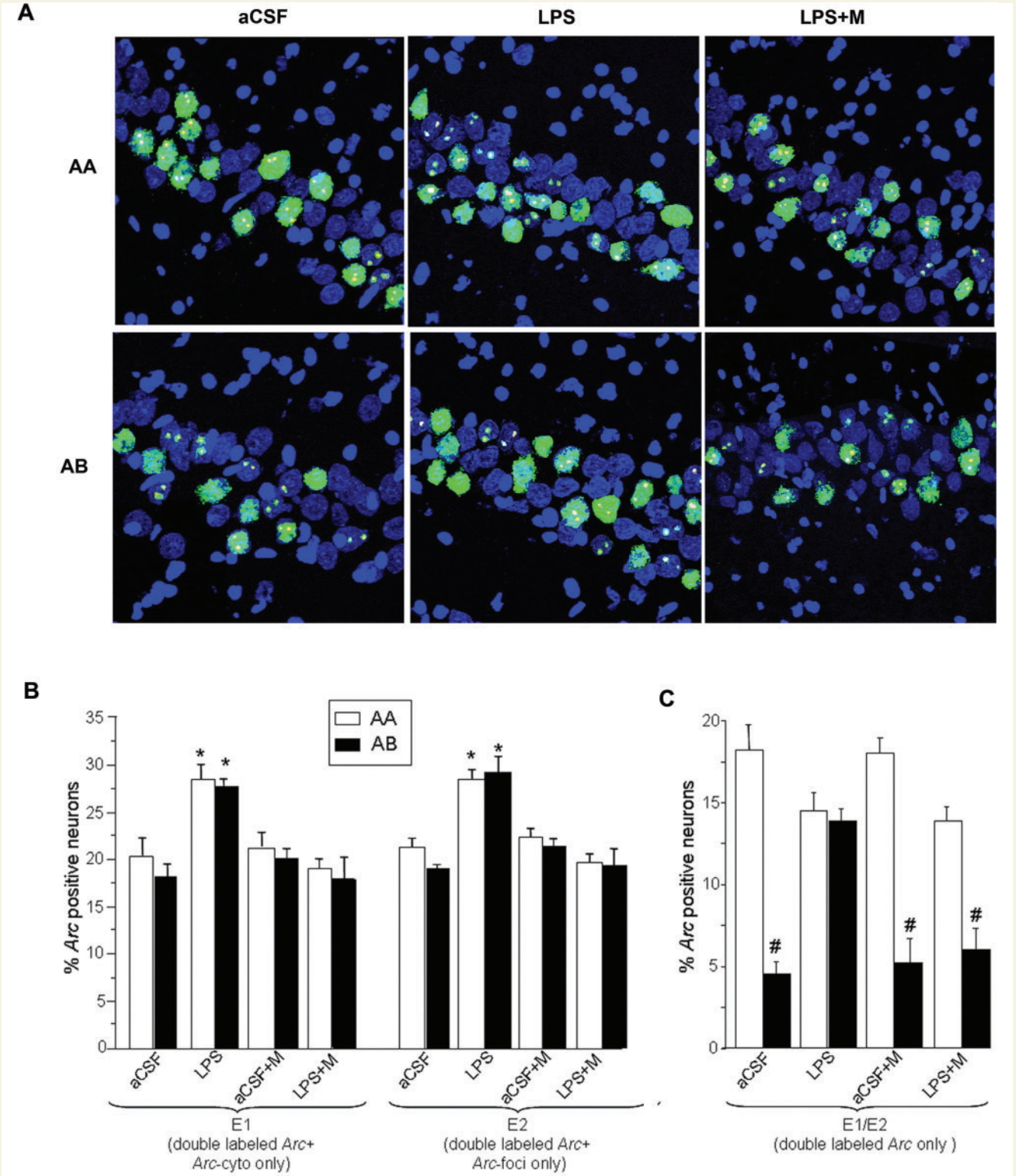

Figure 2 Summary of the *Arc* catFISH data in area CA3. (**A**) Confocal projection images showing *Arc* expression following exploration of either identical (AA, top row) or different (AB, bottom row) environments in three of the treatment groups. Treatment groups included animals chronically infused with artificial cerebrospinal fluid (aCSF); lipopolysaccharide (LPS); LPS and treatment with memantine (LPS+M), and aCSF plus memantine (aCSF + M). Digoxigenin-labelled *Arc*-intron antisense probe was detected with Cy3 (red, see Methods section). Fluorescein-labelled *Arc* antisense full probe was detected with FITC (green, see Methods section), and cell nuclei were counterstained with in blue. The *Arc*-foci appear yellow as a result of the overlap of red (dogoxigenin) and the green FITC-labelled *Arc*. Animals from the aCSF treatment group exposed to the AA exploration condition primarily exhibited neurons stained for both *Arc*-foci and *Arc*-cyto with only a small number of neurons containing *Arc*-cyto or *Arc*-foci only. As expected,

approaching 1 suggest a high degree of overlap in activation patterns, and scores closer to 0 suggest independent populations. For animals infused with artificial cerebrospinal fluid that explored the same environment twice (AA), both CA3 and CA1 cells showed high similarity scores (~0.8), as predicted (Fig. 4A). In contrast, artificial cerebrospinal fluid rats allowed to explore two different environments (AB), showed two statistically independent populations of neurons activated in CA3 and CA1, as evidenced by a low similarity score (~0.2). Similar results were observed for animals infused with artificial cerebrospinal fluid and treated with memantine (Fig. 4A). In lipopolysaccharide-treated animals, however, the CA3 similarity scores for the AA group were significantly lower than for the artificial cerebrospinal fluid-treated animals; the similarity scores for the AB group were higher [ANOVA for CA3: $F(7,38) = 16.5$, $P < 0.05$; for CA1: $F(7,38) = 32.5$, $P < 0.05$; all appropriate *post hoc* comparisons had $P < 0.05$]. Interestingly, in lipopolysaccharide-treated rats, treatment with memantine was able to largely restore the high overlap in the AA condition and lower overlap in the AB treatment group (Fig. 4A). The observed similarities and differences among the groups are best understood via graphical display of the relationship between similarity scores between CA1 and CA3 (Fig. 4B). The distribution of the two populations of animals AA and AB is very well separated with AB close to 0 and AA close to 1 for artificial cerebrospinal fluid and aCSF + M animals (Fig. 4B). After lipopolysaccharide treatment, the distribution of the two populations of animals AA and AB is not well separated in either of the two behavioural conditions. Following the LPS-memantine treatment the distribution of the animals appear more separated. As is shown in Fig. 4B there does not appear to be a strong correlation between CA1 and CA3 similarity scores within animal groups as might be expected from the literature (Vazdarjanova and Guzowski, 2004). The calculated correlation figures are aCSF AA, $R^2 = 0.164$; aCSF AB, $R^2 = 0.347$; LPS AA $R^2 = 0.032$; LPS AB, $R^2 = 0.027$; aCSF + M AA, $R^2 = 0.16$; aCSF + M AB, $R^2 = 0.46$; LPS + M AA, $R^2 = 0.647$; LPS + M AB, $R^2 = 0.363$.

Memantine does not directly affect microglia

Chronic infusion of lipopolysaccharide *in vivo* resulted in the selective activation of microglia within CA3 area and this was significantly reduced with memantine treatment (Fig. 5A and B). To determine if memantine affected microglial activation indirectly through its action on neuronal NMDARs, we employed an *in vitro* system and used quantitative Real Time PCR (qPCR) to examine expression of NMDARs mRNA. Using primers specific for the NR1 subunit of the NMDA receptor, a subunit that is required for formation of a functional channel (Monyer *et al*., 1992), no NMDAR expression was detected in either untreated or LPS-stimulated N9 microglial cells (not shown). Despite the lack of NMDARs, the possibility remained that memantine acted directly on microglial cells to alter their activation state by a mechanism that did not depend on NMDARs. To test this possibility, we cultured N9 microglial cells in the presence of memantine and/or lipopolysaccharide. Treatment with memantine did not result in any changes from control levels (Fig. 6). Treatment with lipopolysaccharide did stimulate these microglial cells to significantly increase transcription of the pro inflammatory mediators Tumor Necrosis Factor α (TNFα) and inducible nitric oxide synthase (iNOS), as measured by qPCR (Fig. 6). When cells were treated with memantine and lipopolysaccharide at the same time, microglial cells increased the transcription of TNFα and iNOS similarly to the lipopolysaccharide treatment alone. Taken together, the data suggest that memantine treatment alone did not directly affect microglial cells.

Discussion

The results of the present experiments provide novel insights into hippocampal network impairment that may underlie the cognitive deficits observed during chronic neuroinflammation. This work relied upon the measurement of the IEG *Arc*, which has been shown to be a reliable monitor of cellular activity reflecting spatial and contextual information processing (Guzowski *et al*., 1999). Two principal findings emerge from these studies. First, following treatment with a proinflammatory agent (LPS), behaviourally driven hippocampal network activity is preserved in CA1 pyramidal cells, but the circuit activation patterns are profoundly disrupted in CA3 cells. Second, memantine, a moderate-affinity uncompetitive open NMDAR channel antagonist, administered concurrently with LPS, is able to preserve normal activity patterns in the CA3 region. A final important observation from these experiments is that the anti-inflammatory effect of memantine appears to be due to its effects on neurons rather than glia. The two observations that support this conclusion are that NMDARs are not observed on microglia and that memantine did not impact the expression of pro-inflammatory genes in cultured microglia (Fig. 6).

when exposed to the AB exploration condition, the aCSF animals showed similar numbers of neurons stained for *Arc*-cyto only, *Arc*-foci only or both. In contrast, animals from the LPS treatment group showed similar population of neurons stained with *Arc*-foci, *Arc*-cyto or both in the AA and the AB exploration conditions. The staining profile observed during treatment with memantine with and without LPS was similar to the aCSF group alone. Scale bar 50 μm. (**B**) In the LPS treatment group, the percentage of neurons activated during epoch 1 (double labelled for *Arc*-cyto/*Arc*-foci plus *Arc*/cyto only) and epoch 2 (double labelled for *Arc*-cyto/*Arc*-foci plus *Arc*/foci only), was significantly higher compared to the aCSF treatment group, (*$P < 0.05$ aCSF AA versus LPS AA, aCSF AB versus LPS AB). (**C**) The percentage of double-labelled neurons (*Arc*-cyto/*Arc*-foci) activated during both epochs 1 and 2. The highest percentage of double-labelled neurons was observed during the AA exploration condition and the lowest during the AB exploration condition in the aCSF, aCSF+M and LPS+M treatment groups. No difference was observed between the exploration condition AA and AB in the LPS treatment group. ($^{\#}P < 0.0001$ AA versus AB for aCSF, LPS and LPS+M group).

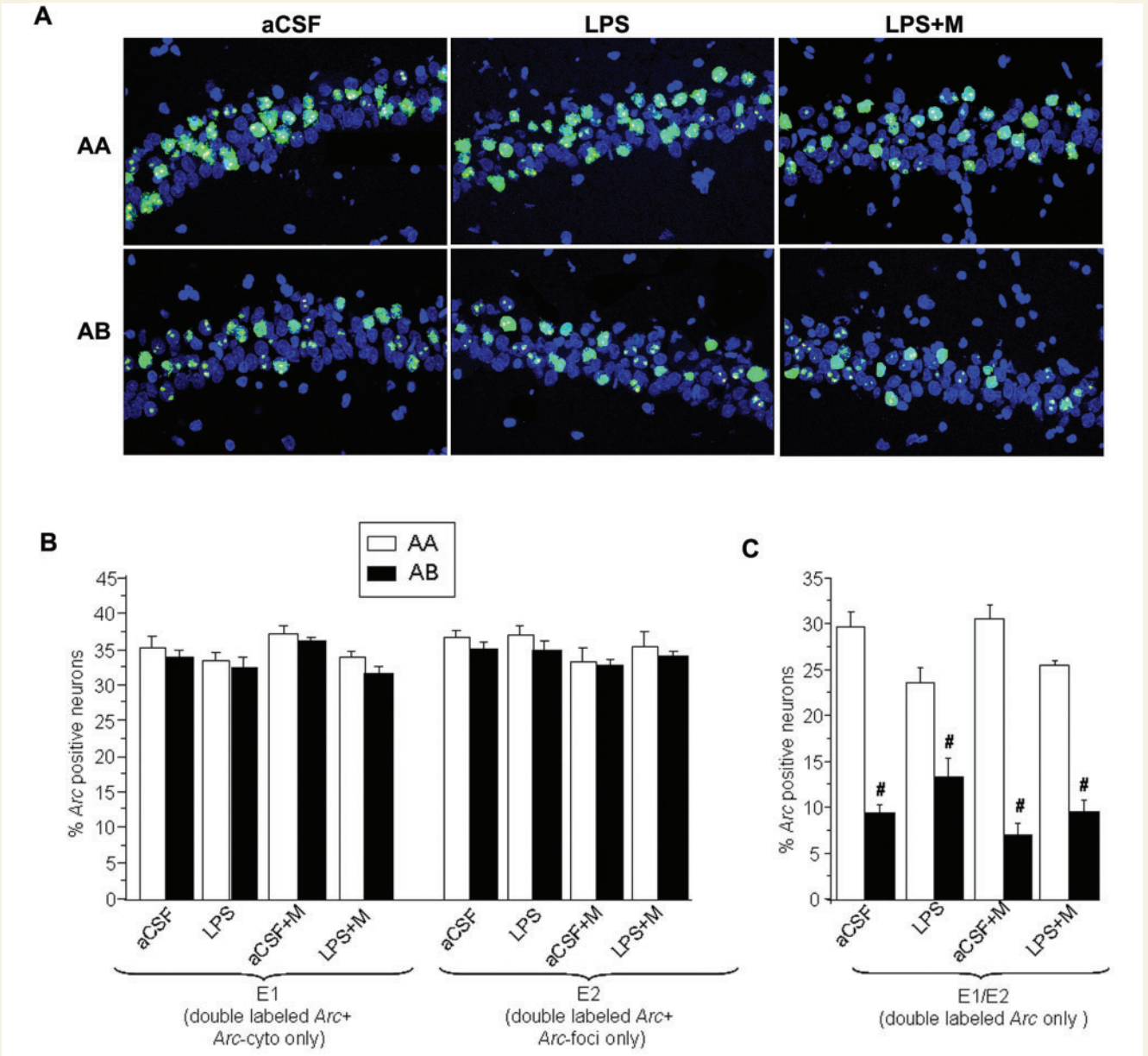

Figure 3 Summary of the *Arc* catFISH data in CA1 area. (**A**) Confocal projection images showing CA1 cell staining profiles detected using *Arc* catFISH following exploration of either identical (AA, top row) or different (AB, bottom row) environments in three of the treatment groups. Treatment groups included animals chronically infused with artificial cerebrospinal fluid (aCSF); aCSF and treatment with memantine (aCSF+M); lipopolysaccharide (LPS); LPS and treatment with memantine (LPS+M). Following the AA exploration condition the majority of the neurons showed double labelling (*Arc*-foci/*Arc*-cyto) and only a small number of neurons contained only *Arc*-cyto or only *Arc*-foci. Conversely, animals exposed to the AB exploration condition showed similar numbers of neurons with *Arc*-cyto only, *Arc*-foci only or both. (**B**) The percentages of *Arc*-positive neurons activated during epochs 1 and 2 were similar in all the treatment conditions. (**C**) The AA exploration condition resulted in the highest percentage of double-labelled neurons (*Arc*-foci/*Arc*-cyto) for all treatments (LPS, LPS+M and aCSF), indicating overlap of neurons activated during epochs 1 and 2. As predicted, the AB exploration condition had lower overlap. ($^{\#}P<0.05$ AB versus AA for aCSF, LPS and LPS+M group) in all treatment conditions.

Spatial information processing accuracy is impaired in the CA3 network during neuroinflammation

Both electrophysiological (Lee *et al*., 2004; Leutgeb *et al*., 2004) and *Arc* catFISH studies (Guzowski *et al*., 2004; Vazdarjanova and Guzowski, 2004) indicate that overlapping CA3 and CA1 neuronal ensembles are activated following two epochs of exploration of the same environment; this represents pattern completion. Furthermore, those studies also indicate that after exploration of two distinct environments, the ensembles engaged in CA3 and CA1 have a low degree of overlap, and thus can be considered to be statistically independent; this represents pattern separation.

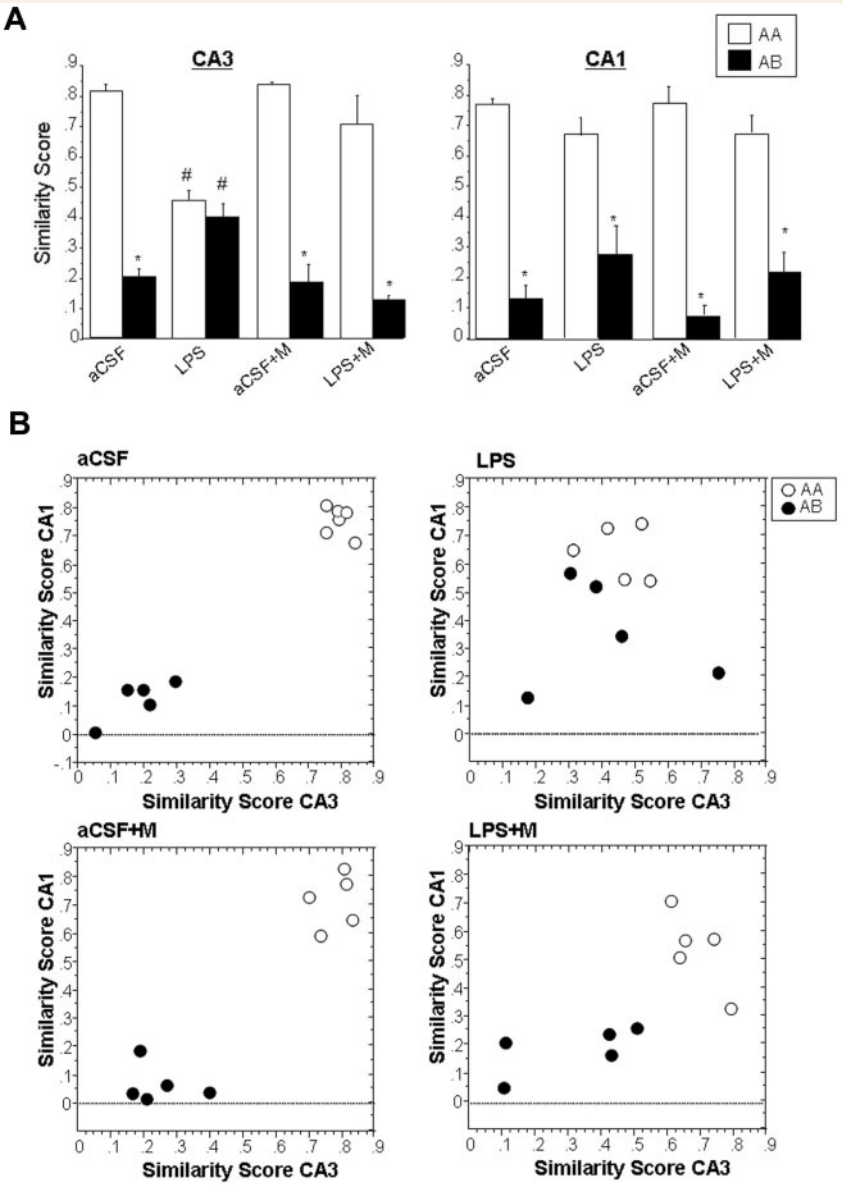

Figure 4 Analysis of CA1 and CA3 neurons activated by epochs 1 and 2 using the similarity score analysis. A similarity score of 1 indicates that the neurons activated during epoch 1 are the same as those activated during epoch 2 (all the neurons are double labelled for *Arc*-foci/*Arc*-cyto). A similarity score of 0 indicates that all the neurons activated during epoch 2 are different from epoch 1, suggesting complete statistical independence of the two populations (see Discussion section). Treatment groups included animals chronically infused with artificial cerebrospinal fluid (aCSF); lipopolysaccharide (LPS); aCSF and treatment with memantine (aCSF+M); LPS treatment with memantine (LPS+M). (**A**) The similarity score for the aCSF treatment group showed high overlap of neurons activated during epochs 1 and 2 in the AA exploration condition, and low overlap of neurons activated in the AB exploration condition in both CA3 and CA1 area. In contrast, LPS treatment resulted in a similar overlap of neurons activated during the two behavioural epochs in both AA and AB conditions only in CA3. This did not occur in the CA1 area. Interestingly, treatment with memantine, was able to largely restore the high overlap in the AA condition and low overlap in AB condition ($^{*}P<0.05$, AA versus AB) in CA3. There was a striking difference in overlap scores between the LPS treatment group compared to aCSF animals ($^{\#}P<0.05$, aCSF AA versus LPS AA, aCSF AB versus LPS AB). (**B**) Correlation analysis between CA3 and CA1 similarity scores for each animal within each treatment and behavioural condition (aCSF AA, $R^2=0.164$; aCSF AB, $R^2=0.027$; LPS AA, $R^2=0.032$; LPS AB, $R^2=0.027$; aCSF+M AA, $R^2=0.016$; aCSF+M AB, $R^2=0.006$; LPS+M AA, $R^2=0.647$; LPS+M AB, $R^2=0.363$). Within each group of animals there was no significant correlation between CA1 and CA3 similarity scores; however, note the large separation between AA and AB in the aCSF and aCSF+M group, and the mixed distribution in the LPS group; the LPS+M group shows a less sparse and more separate distribution of CA1 and CA3 similarity scores.

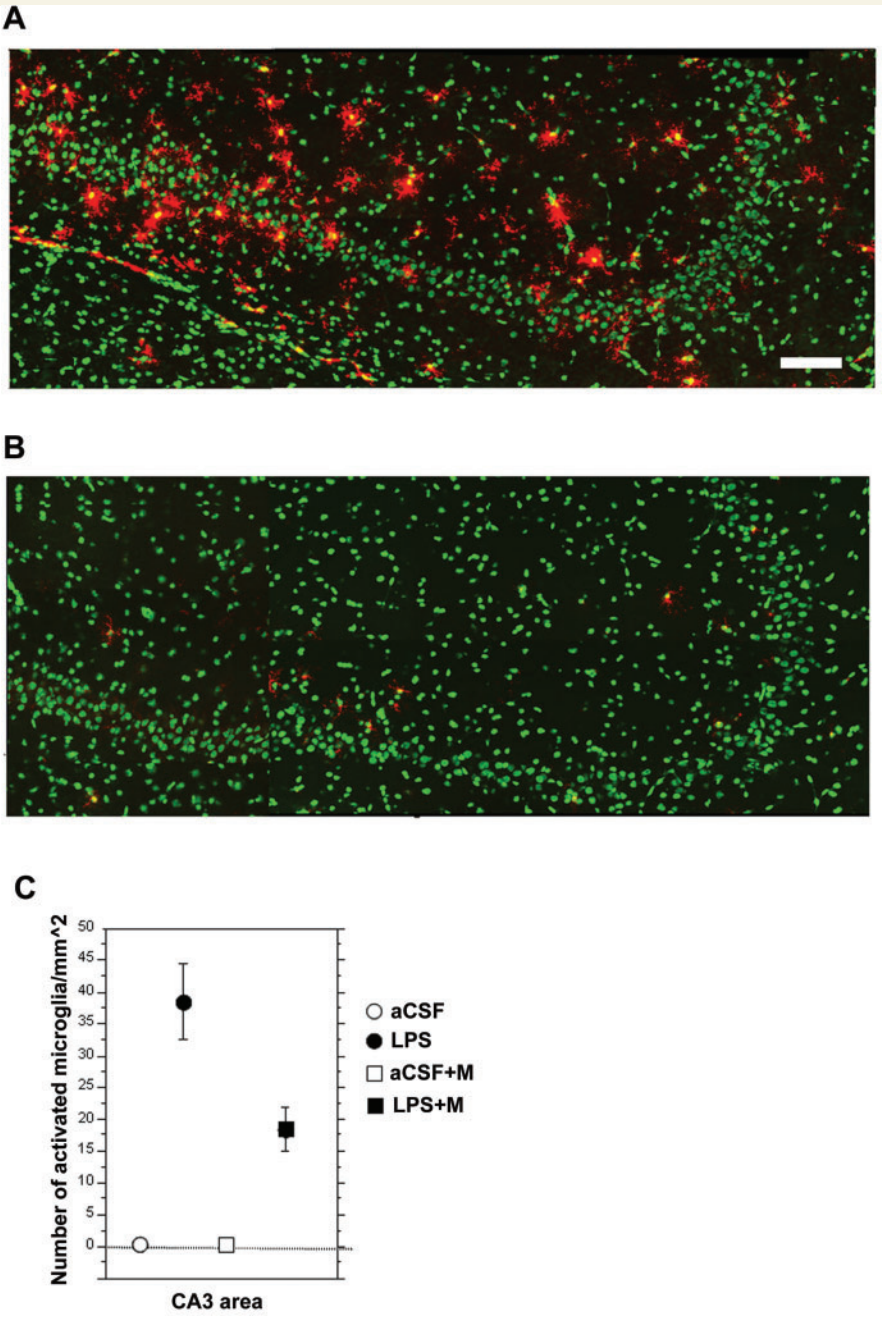

Figure 5 Representative flat images of reconstructed CA3 area from the dorsal hippocampus (~−3.6 mm from bregma) from animals chronically infused with LPS (**A**) and animals chronically infused with LPS and treated with memantine (**B**). Activated microglia are showed in red and nuclei are counterstained in green. Scale bar = 100 μm. As previously reported (Rosi *et al*., 2006) animal infused with LPS that received memantine treatment showed a significant reduction in activated microglia cells/mm^2 in the CA3 area as compared to LPS alone (**C**).

The implication of these data is that the CA3 hippocampal system forms stable, independent neural representations or spatial maps, after a given behavioural experience (Leutgeb *et al*., 2004). In the animals with chronic LPS-induced neuroinflammation, the size of neuronal populations activated in CA3 after exploration was significantly higher (~30%) than that activated in the aCSF-infused control animals (~20%). The reduced sparsity of the CA3 network, which refers to the abnormal number of neurons that are inappropriately activated, may in part explain the cognitive impairment that results from neuroinflammation (Rosi *et al*., 2005). This is supported by modelling studies indicating that associative networks, such as those investigated here, are worse at separating representations that are less sparse, and their mnemonic storage capacity is diminished (McNaughton, 1987; Treves and Rolls, 1992). Here we found direct evidence for this effect, in that neuroinflammation led not only to impaired sparsity

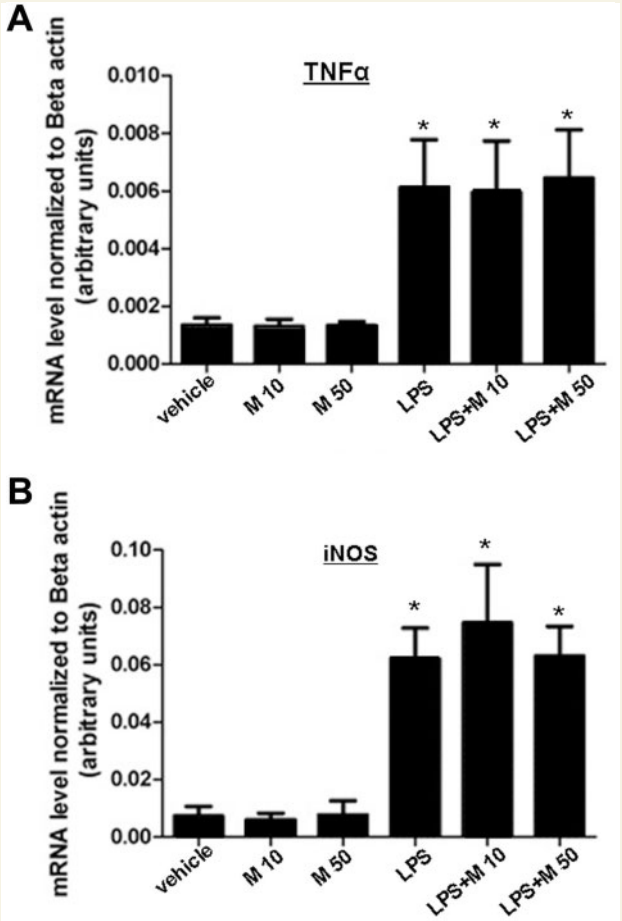

Figure 6 Quantitative real-time PCR (qPCR) analysis of TNFα (**A**) and iNOS mRNA (**B**) levels in cultured N9 microglial cells. Cells treated with LPS for 24 h showed significantly increased expression of both TNFα and iNOS mRNA compared to vehicle (macrophage serum free medium) treated cells. Twenty-four hour of memantine treatment, alone or in combination with LPS treatment, had no effect on gene transcription ($^*P < 0.05$); $n = 4$ for separate experiments, error bars represent SEM.

of CA3 activation (Fig. 2B), but also to the inability of neurons to discriminate different environments which is evident by the lack of pattern separation (Fig. 2C). Moreover, the reduced sparsity most likely reflects representations that are noisier (i.e. that are reactivated with limited consistency across sessions). This noise may be expressed by weaker pattern separation (additional neurons that do not distinguish two distinct environments), and by weaker pattern completion (a different set of additional neurons may be activated when returning to the same environment). Consistent with this interpretation, in LPS-treated rats, the degree of overlap of the CA3 neuronal ensembles during exploration of the same environment (AA) is significantly lower, and during exploration of distinct environments (AB) significantly higher, than that observed in aCSF-AA control animals (Fig. 2C). Dysfunction of pattern separation and completion processes in CA3 may thus impair the normal ability of the system to discriminate two different environments as distinct, and also to ignore small differences in an environment, enabling the recollection that the environment is familiar. This dysfunction can be interpreted as a reduced reliability of information processing in hippocampal networks. Thus, these data are congruent with previously reported studies which showed that during chronic neuroinflammation animals were unable to solve the Morris water maze task (Rosi *et al.*, 2006, Fig. 1A and B). In order to properly solve the Morris water maze task, animals require proper pattern separation and completion (Gilbert *et al.*, 1998; Redish and Touretzky, 1998; Nakazawa *et al.*, 2002). The catFISH methodology provides a unique opportunity to dissect such pattern separation at the cellular level in LPS and LPS + M treated animals.

These results are similar, in some respects, to the changes observed in memory-impaired old animals (Barnes *et al.*, 1997). While neuronal ensemble recordings obtained from freely behaving young rats suggest accurate retrieval of activity patterns in neurons between the first and second of two identical experiences, old rats do not always exhibit such retrieval (Barnes *et al.*, 1997). That is, spatial memory-impaired old rats probabilistically show in CA1 either accurate retrieval (Leutgeb *et al.*, 2004) or global remapping, that is, an activity pattern typical of a different environment condition (AB) even though animals are exposed to the same environment twice (AA) (Barnes *et al.*, 1997). On the other hand, in the CA3 region of old rats, the activity patterns observed after exploration of two different environments is the same as if they were exposed to the same environment twice (AA) (Tanila *et al.*, 1997*a*,*b*; Redish *et al.*, 1998). This dysfunction of hippocampal system computations in ageing has been interpreted as a failure to accomplish pattern completion and pattern separation operations that normally function in this system (Burke and Barnes, 2006). While the changes in normal ageing and under neuroinflammation are distinct, they illustrate how changes in network function can contribute to changes in information processing that can result in cognitive deficits.

CA3 versus CA1 network accuracy

As discussed above, studies in normal animals using both electrophysiological and *Arc* catFISH methods support the idea that CA3 and CA1 perform distinct but complementary functions in the processing of contextual and spatial information (Guzowski *et al.*, 2004; Lee *et al.*, 2004; Leutgeb *et al.*, 2004; Vazdarjanova and Guzowski, 2004). The CA3 network is particularly efficient in performing pattern completion when subtle environmental differences exist, and can perform unambiguous pattern separation when the environmental features are notably distinct (Lee *et al.*, 2004; Vazdarjanova and Guzowski, 2004). The CA1 network, on the other hand, performs pattern separation more gradually, showing partial remapping when subtle changes in environmental features occur (Leutgeb *et al.*, 2004; Vazdarjanova and Guzowski, 2004).

The selective effects on network stability observed in CA3 could result from anatomical and physiological differences between the CA3 and CA1 hippocampal subregions. The present results suggest that CA1 function is intact, in spite of the fact that CA3 operations are disrupted. This indicates that accuracy of

CA1 network function can be independent of the computations performed in CA3. This finding is consistent with the observation that CA1 firing characteristics can be preserved in the face of disrupted CA3 activity following inactivation (McNaughton *et al*., 1989). Additionally, recent results demonstrate that the direct input to the CA1 received from entorhinal cortical layer III neurons (Brun *et al*., 2008) contributes significantly to information processing in CA1.

Memantine treatment partially restores the accuracy of information processing in the hippocampus

Treatment with memantine, a low-to-moderate affinity open-channel non-competitive NMDARs antagonist (Parsons *et al*., 1999; Danysz and Parsons, 2003), was able to counteract the effect of chronic lipopolysaccharide treatment at least in terms of the accuracy of spatial information processing in CA3. While treatment with memantine alone did not affect activity in CA1 or CA3, animals with chronic neuroinflammation treated with memantine did activate highly overlapping neuronal ensembles during exploration of two identical environments, and largely independent populations of neurons following exploration of two distinct environments. Thus, pattern completion and separation operations were normalized by the memantine treatment in animals subjected to lipopolysaccharide infusion. The mechanism underling memantine's effect on information processing may involve postsynaptic calcium entry in the presence of elevated extracellular glutamate. This could develop in response to the pro-inflammatory environment produced by lipopolysaccharide. Consistent with this hypothesis is the fact that *Arc* expression is NMDAR-dependent and memantine is known to act only on open NMDAR channels inhibiting inward depolarizing currents (Danysz and Parsons, 2003).

There were differences between CA3 and CA1 information processing that may be important in explaining the effect of memantine on the behavioural performance of LPS-treated animals. The similarity score analyses confirm that lipopolysaccharide animals showed a pronounced decrease in the accuracy of the hippocampal CA3 network as compared to the other experimental groups. Interestingly, the similarity scores between CA3 and CA1 in the AA and AB groups are distinctly different (Fig. 4) in the aCSF and aCSF + M groups, indicating that under normal conditions the computations performed by the CA3 and the CA1 networks are congruent with each other. In contrast, the similarity score between these hippocampal regions in the LPS-treated animals are not distinct, revealing incongruent computations performed in these two hippocampal regions in animals with neuroinflammation. It is noteworthy that for lipopolysaccharide animals treated with memantine, similarity scores for CA3 and CA1 showed greater separation between the AA and AB condition, compared to lipopolysaccharide alone, but were intermediate relative to that observed in artificial cerebrospinal fluid controls ± memantine. This suggests that, although memantine treatment tends to restore network activity patterns within CA3, it does not completely restore the congruence of information processing between CA3 and CA1 regions in lipopolysaccharide infused animals. Although the observed defect is subtle, this may explain why, even when the number of behaviourally activated cells is restored, the performance of lipopolysaccharide memantine-treated animals in the Morris water maze task is only partially improved (Rosi *et al*., 2006, Fig. 1A and B). This suggests that even if CA1 and CA3 can perform their computations independently, the integration of information between the two hippocampal subregions is important for optimal spatial performance.

Activated microglia and information processing in the hippocampus

Previously it was shown that *Arc* expression in CA3 and CA1 was related to the presence (CA3) or absence (CA1) of activated microglia (Rosi *et al*., 2005). In the present study, we have extended this observation by showing that information processing in CA3 was disrupted, while it remained accurate in CA1. Memantine decreased the number of activated microglia in CA3 (Fig. 5) and also largely restored the accuracy of information processing in that region, but there were no discernible effects in CA1. This suggests that at least for CA3, the presence of activated microglia has a negative impact on information processing.

How memantine restores accuracy of information processing and, ultimately, memory, during neuroinflammation is not known. One possibility is that it acts on NMDARs expressed by microglia, and another is that it acts directly on neuronal NMDAR. Support for the first possibility is that the presence of activated microglia correlates both with impaired memory and accuracy of information processing (Rosi *et al*., 2005, 2006). Additionally, it has been recently suggested that memantine may act via non-neuronal NMDARs in the developing brain (Manning *et al*., 2008). However, there are currently no data reporting NMDARs expression on adult microglia. Here we provide support for the second possibility, by demonstrating that even when stimulated with lipopolysaccharide, microglia do not express NMDARs. Furthermore, memantine does not influence the activation of untreated or LPS-treated microglial cells in culture. These findings support the idea that memantine modulates NMDARs on neurons. This mechanism may underlie its anti-inflammatory action and may be responsible for its ability to restore hippocampal function and spatial cognitive performance. The implication of these data is that activated microglia indirectly disrupt neuronal information processing. The possible role of activated microglia on neuronal activity and vice versa has been, and is, the focus of several recent studies (de Jong *et al*., 2005; Biber *et al*., 2007, 2008; de Haas *et al*., 2007).

Chronically activated microglia release proinflammatory cytokines and nitric oxide, which in turn leads to a cascade of cellular events including blockage of glutamate reuptake (Robinson *et al*., 1993), and increased synthesis of glutamate by astrocytes (Bezzi *et al*., 1998). The excess extracellular glutamate induced by neuroinflammation (Fine *et al*., 1996) may result in an excess of calcium entry in the postsynaptic neurons leading to

a positive feedback toxic cycle in which activated microglia release inflammatory mediators such as cytokines (Bezzi *et al*., 2001). Furthermore, elevated levels of glutamate may act on non-NMDARs and cause chronic membrane depolarization that would partially relieve the voltage-dependent Mg^{2+} block of the NMDARs. It is possible that subsequent activation of NMDARs by ordinary glutamatergic synaptic activity may thus permit a continuous influx of Ca^{2+} ions into the neurons; at this time this is only speculative. However, under this scenario, CA3 pyramidal neurons would be unable to discriminate signals coming from the mossy fibres and perforant path. The inflammation-induced threshold change for neuronal activation (i.e. *Arc* expression), may therefore reflect the observed altered pattern completion and separation processes, and may be influenced by elevated levels of cytokines and/or nitric oxide. Furthermore, elevated levels of inflammatory cytokines enhance the NMDA-dependent intracellular calcium levels (Viviani *et al*., 2003). Given that memantine promotes the normal entry of calcium through NMDARs, this could help explain how this agent stabilizes neuronal signalling.

Therefore, during the early stages of neuroinflammation, dysfunction at the NMDA-glutamate synapse may disrupt accuracy of information processing, while in the later stages this condition may contribute to neuronal degeneration. Overall, given the role of activated microglia on neuronal activity and *vice versa* (de Jong *et al*., 2005; Biber *et al*., 2007, 2008; de Haas *et al*., 2007), it is possible that the specificity of the deficit is due to this microglial activation and its effect on CA3 pyramidal cell function. The direct input from the entorhinal cortex to CA1, on the other hand, may allow relatively normal activity to occur in the CA1 pyramidal cells, in spite of the altered input from CA3.

While it is not possible to definitively answer the question of whether memantine acts via principal cells or interneuron NMDARs (or both), recent data concerning this topic suggest that it is less likely to work through alterations of interneuron function. Computational models of hippocampal function (Treves and Rolls, 1992) have shown that efficient pattern separation requires parallel activation of two excitatory inputs to CA3, the perforant path from layer two of the entorhinal cortex and the granule cell axons (mossy fibres, MF). When multiple cortical input patterns to CA3 arrive simultaneously, feed forward inhibition driven by mossy fibres limit the number of pyramidal cells activated by the same input. This further increases the sparsity of the network and the storage capacity in the CA3 (Treves and Rolls, 1992). Thus, the CA3 feed forward inhibitory interneurons may play a role in regulating decorrelation of compressed memory representations in CA3 area. Furthermore, it has been demonstrated that the inhibitory interneurons express LTP that contributes to hippocampal network plasticity. This plasticity, however, is independent of NMDAR, and dependent on metabotropic glutamate receptors (Perez *et al*., 2001; Galvan *et al*., 2008). Given these data it is possible that the changes observed during neuroinflammation and treatment with memantine at the dose used here, are mostly mediated via principal cell NMDARs. Future work will elucidate the precise mechanisms guiding these processes.

Conclusions

We have demonstrated that LPS-induced neuroinflammation disrupts accuracy of information processing in the hippocampus and that this disruption is partially normalized by co-administration of memantine. Memantine appears to exert its effect by acting directly on neuronal NMDARs, and not on microglia themselves. Thus, memantine treatment given early in the progression of neurodegenerative diseases may confer neuronal and cognitive protection by conserving accurate information processing and indirectly preventing pathological microglia activation.

Acknowledgements

We would like to thank Dr Alessandro Treves for his critical feedback on the article and Dr Kathleen Lamborn for her help with the data analysis.

Funding

National Institutes of Health (AG009219 to C.A.B.; AG10546 to G.L.W.; AG030331 to G.L.W.); McKnight Brain Research Foundation state of Arizona and Arizona Department of Health Services (to C.A.B.); Consejo Nacional de Ciencia y Tecnologia (51028 to V.R.A); Direccion General de Asuntos del Personal Academico UNAM (IN213907 to V.R.A.).

References

Akiyama H, Barger S, Barnum S, Bradt B, Bauer J, Cole GM, et al. Inflammation and Alzheimer's disease. Neurobiol Aging 2000; 21: 383–421.

Barger SW, Basile AS. Activation of microglia by secreted amyloid precursor protein evokes release of glutamate by cystine exchange and attenuates synaptic function. J Neurochem 2001; 76: 846–54.

Barnes CA, Suster MS, Shen J, McNaughton BL. Multistability of cognitive maps in the hippocampus of old rats. Nature 1997; 388: 272–5.

Bezzi P, Carmignoto G, Pasti L, Vesce S, Rossi D, Rizzini BL, et al. Prostaglandins stimulate calcium-dependent glutamate release in astrocytes. Nature 1998; 391: 281–5.

Bezzi P, Domercq M, Brambilla L, Galli R, Schols D, De Clercq E, et al. CXCR4-activated astrocyte glutamate release via TNFalpha: amplification by microglia triggers neurotoxicity. Nat Neurosci 2001; 4: 702–10.

Biber K, Neumann H, Inoue K, Boddeke HW. Neuronal 'on' and 'off' signals control microglia. Trends Neurosci 2007; 30: 596–602.

Biber K, Vinet J, Boddeke HW. Neuron-microglia signaling: chemokines as versatile messengers. J Neuroimmunol 2008; 198: 69–74.

Brun VH, Leutgeb S, Wu HQ, Schwarcz R, Witter MP, Moser EI, et al. Impaired spatial representation in CA1 after lesion of direct input from entorhinal cortex. Neuron 2008; 57: 290–302.

Burke SN, Barnes CA. Neural plasticity in the ageing brain. Nat Rev Neurosci 2006; 7: 30–40.

Cagnin A, Brooks DJ, Kennedy AM, Gunn RN, Myers R, Turkheimer FE, et al. In-vivo measurement of activated microglia in dementia. Lancet 2001; 358: 461–7.

Danysz W, Parsons CG. The NMDA receptor antagonist memantine as a symptomatological and neuroprotective treatment for

Alzheimer's disease: preclinical evidence. Int J Geriatr Psychiatry 2003; 18: S23–32.

de Haas AH, van Weering HR, de Jong EK, Boddeke HW, Biber KP. Neuronal chemokines: versatile messengers in central nervous system cell interaction. Mol Neurobiol 2007; 36: 137–51.

de Jong EK, Dijkstra IM, Hensens M, Brouwer N, van Amerongen M, Liem RS, et al. Vesicle-mediated transport and release of CCL21 in endangered neurons: a possible explanation for microglia activation remote from a primary lesion. J Neurosci 2005; 25: 7548–57.

Fine SM, Angel RA, Perry SW, Epstein LG, Rothstein JD, Dewhurst S, et al. Tumor necrosis factor alpha inhibits glutamate uptake by primary human astrocytes. Implications for pathogenesis of HIV-1 dementia. J Biol Chem 1996; 271: 15303–6.

Fischer-Smith T, Croul S, Adeniyi A, Rybicka K, Morgello S, Khalili K, et al. Macrophage/microglial accumulation and proliferating cell nuclear antigen expression in the central nervous system in human immunodeficiency virus encephalopathy. Am J Pathol 2004; 164: 2089–99.

Galvan EJ, Calixto E, Barrionuevo G. Bidirectional Hebbian plasticity at hippocampal mossy fiber synapses on CA3 interneurons. J Neurosci 2008; 28: 14042–55.

Gilbert PE, Kesner RP, DeCoteau WE. Memory for spatial location: role of the hippocampus in mediating spatial pattern separation. J Neurosci 1998; 18: 804–10.

Guzowski JF, Knierim J, Moser EI. Ensemble dynamics of hippocampal regions CA3 and CA1. Neuron 2004; 18: 581–4.

Guzowski JF, Lyford GL, Stevenson GD, Houston FP, McGaugh JL, Worley PF, et al. Inhibition of activity-dependent arc protein expression in the rat hippocampus impairs the maintenance of long-term potentiation and the consolidation of long-term memory. J Neurosci 2000; 20: 3993–4001.

Guzowski JF, McNaughton BL, Barnes CA, Worley PF. Environment-specific expression of the immediate-early gene Arc in hippocampal neuronal ensembles. Nat Neurosci 1999; 2: 1120–4.

Guzowski JF, Miyashita T, Chawla MK, Sanderson J, Maes LI, Houston FP, et al. Recent behaviour al history modifies coupling between cell activity and Arc gene transcription in hippocampal CA1 neurons. Proc Natl Acad Sci USA 2006; 103: 1077–82.

Lee I, Rao G, Knierim JJ. A double dissociation between hippocampal subfields: differential time course of CA3 and CA1 place cells for processing changed environments. Neuron 2004; 42: 803–15.

Leutgeb S, Leutgeb JK, Treves A, Moser MB, Moser EI. Distinct ensemble codes in hippocampal areas CA3 and CA1. Science 2004; 305: 1295–8.

Lyford GL, Yamagata K, Kaufmann WE, Barnes CA, Sanders LK, Copeland NG, et al. Arc, a growth factor and activity-regulated gene, encodes a novel cytoskeleton-associated protein that is enriched in neuronal dendrites. Neuron 1995; 14: 433–45.

Manning SM, Talos DM, Zhou C, Selip DB, Park HK, Park CJ, et al. NMDA receptor blockade with memantine attenuates white matter injury in a rat model of periventricular leukomalacia. J Neurosci 2008; 28: 6670–8.

McGeer EG, McGeer PL. The importance of inflammatory mechanisms in Alzheimer disease. Exp Gerontol 1998; 33: 371–8.

McNaughton BL, Barnes CA, Meltzer J, Sutherland RJ. Hippocampal granule cells are necessary for normal spatial learning but not for spatially-selective pyramidal cell discharge. Exp Brain Res 1989; 76: 485–96.

McNaughton BL, MR. Hippocampal synaptic enhancement and information storage within distributed memory system. Trends Neurosci 1987; 10: 408–15.

Monyer H, Sprengel R, Schoepfer R, Herb A, Higuchi M, Lomeli H, et al. Heteromeric NMDA receptors: molecular and functional distinction of subtypes. Science 1992; 256: 1217–21.

Morganti-Kossmann MC, Rancan M, Otto VI, Stahel PF, Kossmann T. Role of cerebral inflammation after traumatic brain injury: a revisited concept. Shock 2001; 16: 165–77.

Nakazawa K, Quirk MC, Chitwood RA, Watanabe M, Yeckel MF, Sun LD, et al. Requirement for hippocampal CA3 NMDA receptors in associative memory recall. Science 2002; 297: 211–8.

Parsons CG, Danysz W, Quack G. Memantine is a clinically well tolerated N-methyl-D-aspartate (NMDA) receptor antagonist—a review of preclinical data. Neuropharmacology 1999; 38: 735–67.

Perez Y, Morin F, Lacaille JC. A hebbian form of long-term potentiation dependent on mGluR1a in hippocampal inhibitory interneurons. Proc Natl Acad Sci USA 2001; 98: 9401–6.

Plath N, Ohana O, Dammermann B, Errington ML, Schmitz D, Gross C, et al. Arc/Arg3.1 is essential for the consolidation of synaptic plasticity and memories. Neuron 2006; 52: 437–44.

Ramirez-Amaya V, Vazdarjanova A, Mikhael D, Rosi S, Worley PF, Barnes CA. Spatial exploration-induced Arc mRNA and protein expression: evidence for selective, network-specific reactivation. J Neurosci 2005; 25: 1761–8.

Redish AD, McNaughton BL, Barnes CA. Reconciling Barnes *et al*. (1997) and Tanila *et al*. (1997a,b). Hippocampus 1998; 8: 438–43.

Redish AD, Touretzky DS. The role of the hippocampus in solving the Morris water maze. Neural Comput 1998; 10: 73–111.

Robinson MB, Djali S, Buchhalter JR. Inhibition of glutamate uptake with L-trans-pyrrolidine-2,4-dicarboxylate potentiates glutamate toxicity in primary hippocampal cultures. J Neurochem 1993; 61: 2099–103.

Rosi S, Ramirez-Amaya V, Vazdarjanova A, Worley PF, Barnes CA, Wenk GL. Neuroinflammation alters the hippocampal pattern of behaviour ally induced Arc expression. J Neurosci 2005; 25: 723–31.

Rosi S, Vazdarjanova A, Ramirez-Amaya V, Worley PF, Barnes CA, Wenk GL. Memantine protects against LPS-induced neuroinflammation, restores behaviour ally-induced gene expression and spatial learning in the rat. Neuroscience 2006; 142: 1303–15.

Tanila H, Shapiro M, Gallagher M, Eichenbaum H. Brain aging: changes in the nature of information coding by the hippocampus. J Neurosci 1997a; 17: 5155–66.

Tanila H, Sipila P, Shapiro M, Eichenbaum H. Brain aging: impaired coding of novel environmental cues. J Neurosci 1997b; 17: 5167–74.

Treves A, Rolls ET. Computational constraints suggest the need for two distinct input systems to the hippocampal CA3 network. Hippocampus 1992; 2: 189–99.

Vazdarjanova A, Guzowski JF. Differences in hippocampal neuronal population responses to modifications of an environmental context: evidence for distinct, yet complementary, functions of CA3 and CA1 ensembles. J Neurosci 2004; 24: 6489–96.

Viviani B, Bartesaghi S, Gardoni F, Vezzani A, Behrens MM, Bartfai T, et al. Interleukin-1beta enhances NMDA receptor-mediated intracellular calcium increase through activation of the Src family of kinases. J Neurosci 2003; 23: 8692–700.